Matrix-isolation infrared spectra of 2-, 3- and 4-pyridinecarboxaldehyde before and after UV irradiation

Keiichi Ohno[1)*], Takao Itoh[2)], Chiyumi Yokota[1)] and Yukiteru Katsumoto[1)]

[1)] *Department of Chemistry, Graduate School of Science, Hiroshima University, 1-3-1 Kagamiyama, Higashi-Hiroshima City, 739-8526, Japan*

[2)] *Graduate School of Integrated Arts and Sciences, Hiroshima University, 1-7-1 Kagamiyama, Higashi-Hiroshima City, 739-8521, Japan*

* To whom the correspondence should be addressed.

E-mail: kohno@sci.hiroshima-u.ac.jp (K. Ohno)

Abstract

Three structural isomers of pyridinecarboxaldehydes (2-, 3- and 4-pyridinecarboxaldehyde) have been investigated in detail with matrix-isolation infrared spectroscopy in the 3000–600 cm^{-1} region, combined with the UV photoexcitation and the density-functional theory (DFT) calculations. Two rotamers (anti and syn) were identified for 2- and 3-pyridinecarboxaldehyde (2- and 3-PCA, respectively) upon the photoexcitation and most of the observed bands of each rotamer have been assigned. Both of the infrared data and the results of the DFT calculations strongly support that the syn rotamer exists as a less stable isomer for 2- and 3-PCA. It is shown that the formation of the intramolecular C–H···N hydrogen bond for the anti rotamer of 2-PCA results in the shortening of the aldehyde C–H bond length, while for the syn rotamer the C=O bond length is shortened due to the repulsion between the N and aldehyde O atoms. With 2-PCA, the photoinduced rotational isomerism and photolysis were observed simultaneously upon the UV irradiation.

Keywords: 2-, 3- and 4-Pyridinecarboxaldehyde, Rotamer, Matrix-isolation infrared spectroscopy, UV photoexcitation, Energetics, Density-functional theory calculation

1. Introduction

There are two planar rotational isomers (rotamers) for 2- and 3-pyridinecarboxaldehyde (2-PCA and 3-PCA, respectively) among the three structural isomers, 2-PCA, 3-PCA and 4-pyridinecarboxaldehyde (4-PCA) as are illustrated in Fig. 1. The evidence for the coexistence of the two rotational isomers has been indicated not only by NMR and dipole moment measurements [1–4] but also by *ab initio* calculation using the minimal STO-3G basis set [5]. However, the definite spectroscopic identification and assignments have not been made for the two rotamers of 2- and 3-PCA. Further, only a small number of the spectroscopic data are available in the literatures for pyrimidinecarboxaldehydes. In a foregoing paper, we have obtained clear evidence for the coexistence of the two rotamers of 2- and 3-fluorobenzaldehyde through matrix-isolation infrared-spectral measurements [6] and assigned most of the observed infrared bands of each rotamer. We could have obtained the details of the energetics and populations as well as the infrared feature of each rotamer for fluorobenzaldehydes. Thus, it must be of interest to investigate the similar molecules to obtain further a deeper insight into the relative energies and characteristics of the rotamers and to find common feature of each rotamer.

In the present study, we have measured infrared spectra of 2-, 3- and 4-pyridinecarboxaldehyde (2-, 3- and 4-PCA, respectively) in a low-temperature argon matrix. The coexistence of the anti and syn rotamers has been confirmed for 2- and 3-PCA through the matrix-isolation infrared spectroscopy combined with the UV photoexcitation as well as the density functional calculations, and most of the observed bands for each rotamer have been assigned. Both of the anti and syn rotamers were observed for 3-PCA in the Ar matrix immediately after the deposition, while only the anti rotamer was observed for 2-PCA. Both of the infrared data and the results of the DFT calculations strongly support that the syn rotamer exists as a less stable isomer for 2- and 3-PCA. The aldehyde C–H wavenumber also has been examined to clarify the characteristic tendency of the intramolecular C–H···N hydrogen bond of the anti rotamer of 2-PCA. It is shown that the formation of the intramolecular C–H···N hydrogen bond for the anti rotamer of 2-PCA results in the shortening of the aldehyde C–H bond length, which gives rise to a blue-shift of the C–H stretching band. The comparison of the data for 2-PCA with those for 3- and 4-PCA shows that the C=O bond length is shortened for the syn rotamer of 2-PCA, which is presumably caused by the repulsion between the aldehyde O and N atoms. It is also shown for 2-PCA that the photoinduced rotational isomerism accompanies the photolysis to yield pyridine and

carbon monoxide.

2. Experimental and Calculation Methods

2-, 3- and 4-Pyridinecarboxaldehyde obtained from Aldrich, USA was purified by means of trap-to-trap distillations under vacuum. Each of these samples was diluted with pure argon gas obtained from Nippon Sanso, Japan (99.9999 % purity) to be about 1/800, and was slowly sprayed onto a CsI plate cooled by a closed cycled helium refrigerator (Iwatani, CryoMini D510) to about 15 K. The temperature of the Ar matrix was controlled by a thermostabilizer (Iwatani, TCU-4) using a PID action method and was monitored continuously by an Au-Chromel thermocouple. Infrared absorption spectra of pyridinecarboxaldehydes were measured with a JASCO FT/IR-615 Fourier transform spectrophotometer equipped with a MCT detector. The infrared spectra were obtained by coaddition of 100 scans with a resolution of 1.0 cm^{-1}. In the sample condition mentioned above, the populations of the rotamers frozen at 15 K just after the deposition can be assumed to be the same as those at the temperature of the gaseous sample just before the deposition [7–8]. The effect of photoexcitation was examined by irradiating the UV light to the deposited samples for 10 min. A superhigh-pressure mercury lamp (Ushio, SX-UI 501HQ) was used as a UV light source combined with a water filter to avoid thermal radiation and short-wavelength cutoff filters, Sigma UTF-30U (λ > 300 nm), UTF-34U (λ > 340 nm), UTF-37U (λ > 370 nm) and UTF-42U (λ > 420 nm).

The quantum chemical calculations were carried out using the GAUSSIAN 03 program [9]. Optimized geometries, harmonic wavenumbers and infrared intensities of 2-, 3- and 4-PCA were obtained by density-functional theory (DFT) calculations using the 6-311++G(3df,2pd) basis set. We have used Becke's three-parameter exchange functional [10] for the DFT calculations, together with the correlation functionals of Lee-Yang-Parr (B3LYP) [11]. The harmonic wavenumbers ν_{harm} were scaled by the wavenumber-linear scaling (WLS) method, $\nu_{calc} = \nu_{harm} \times (0.9766 + 0.00000202 \times \nu_{harm})$, to reproduce well the observed bands in the region below 1800 cm^{-1} [12].

3. Results and Discussion

The optimized geometries of the two rotamers of 2- and 3-PCA obtained by the

calculations at the B3LYP/6-311++G(3df,2pd) level are shown in Fig. 1, together with that of 4-PCA. Each of the optimized geometries is planar with the C_s symmetry, which is the same as that determined by microwave spectroscopy for the anti rotamer of 2-PCA [13]. The 33 fundamentals are divided into 23 of the a′ species (in-plane modes) and 10 of the a″ species (out-of-plane modes) for each of 2-, 3- and 4-PCA. The observed and scaled harmonic wavenumbers, ν_{calc}, of 2-, 3- and 4-PCA in the 1800–600 cm^{-1} region are given in Tables 1–3, respectively, along with the brief assignments. In Table 4 we show the observed and scaled harmonic wavenumbers of the aldehyde C–H stretching in the 3000–2700 cm^{-1} region.

3. 1. Infrared-band assignments

Green and Harrison have reported the infrared spectra of liquid 2-, 3- and 4-PCA and assigned the spectra of 2- and 3-PCA as those of the major rotamer of anti [14]. In Fig. 2 we show the observed and calculated matrix-isolation infrared spectra of 4-PCA whose wavenumbers are quite similar to those reported previously in the liquid phase [14]. The observed spectra in the 1900–700 cm^{-1} region are reproduced well within 27 cm^{-1} using the wavenumbers and intensities calculated at the B3LYP/6-311++G(3df,2pd) level, except for the 1623 and 1608 cm^{-1} bands due to water as well as for the 1200 cm^{-1} band. The 1200 cm^{-1} band, which is intensified by Fermi resonance with the fundamental band at 1191 cm^{-1}, may be assigned to the combination band (989 + 210) [14]. The weakly observed shoulder bands may be due to the site effect of the argon matrix [15] or due to aggregation products such as dimer.

In Fig. 3 we show observed and calculated matrix-isolation infrared spectra of 3-PCA, where the downward and upward bands of the calculated spectrum are those of the anti and syn rotamers, respectively. The infrared spectrum measured immediately after the deposition (Fig. 3a) shows the feature of both the anti and syn rotamers of 3-PCA. Fig. 3b shows the observed difference spectrum of 3-PCA, where the spectrum obtained before the UV irradiation shown in Fig. 3a is subtracted from that obtained after the UV irradiation; that is, the downward and upward bands are associated, respectively, with the bands decreased and increased upon the UV irradiation. Thus, each band of the anti and syn rotamers of 3-PCA was detected separately upon the UV irradiation of the deposited samples. It is inferred from the comparison of the calculated spectra (Fig. 3c) with the observed spectra (Fig. 3b) that the bands decreased (downward bands) and increased (upward bands) upon the UV irradiation are due to the anti and syn rotamers of 3-PCA, respectively. The results of calculations at the B3LYP/6-311++G(3df,2pd) level show that the anti rotamer is

slightly stable by 2.8 kJ mol^{-1} (234 cm^{-1}) as compared with the syn rotamer, indicating that the population ratio of syn/anti is 0.32 at 294 K. This energy difference is in agreement with that reported previously using NMR and dipole-moment techniques: 3-PCA at room temperature is reported to be an equilibrium of 20–30 % syn and 70–80 % anti [1,3,4]. The barrier height from the anti to the syn rotamer is calculated to be 33.5 kJ mol^{-1} (2800 cm^{-1}), indicating that the conversion between the anti and syn rotamers is not expected to occur at 15 K [16]. This height is in good agreement with that obtained in CHF_2Cl solution using NMR technique (32.1 kJ mol^{-1} (2683 cm^{-1})) [1].

Figure 4 shows observed and calculated matrix-isolation infrared spectra of 2-PCA, where the downward and upward bands of the calculated spectrum correspond to those of the anti and syn rotamers, respectively. The infrared spectrum measured just after the deposition (Fig. 4a) shows that most of the bands are due to the anti rotamer. The present result for 2-PCA is in agreement with that obtained previously with MW, NMR and dipole-moment measurements, although a fairly large amount of the syn rotamer has been deduced from the MNR measurement, which has been presumably caused by the solvent effect [1–4]. The result of the NMR measurement has shown that the anti rotamer is more stable than the syn rotamer by at least 9.6 kJ mol^{-1} in CS_2 solution [3]. Fig. 4b shows the difference spectrum of 2-PCA, where the spectrum obtained before the UV irradiation shown in Fig. 4a are subtracted from that obtained after the UV irradiation. The comparison of the calculated spectrum with the observed spectrum shows that the bands decreased and increased upon the UV irradiation are, respectively, due to the anti and syn rotamers of 2-PCA, except for several upward bands assigned to pyridine which is formed as the result of the photolysis of the parent molecule. The result of the calculations at the B3LYP/6-311++G(3df,2pd) level shows that the anti rotamer is more stable than the syn rotamer by 17.1 kJ mol^{-1} (1430 cm^{-1}), indicating that the population ratio of anti/syn is 1/0.001 at 294 K. This fairly large energy difference between the two rotamers is presumably, in one hand, due to the stabilization of the intramolecular C–H···N hydrogen bond of the anti rotamer, but on the other hand due to the destabilization of the repulsion between the N and aldehyde O atoms of the syn rotamer. The barrier height from the anti to the sym rotamer is calculated to be 36.1 kJ mol^{-1} (3018 cm^{-1}) for 2-PCA.

UV irradiation ($\lambda > 300$ nm) of the samples deposited at 15 K yields an increase of the population of the less stable rotamer for both of 2- and 3-PCA. Hence, the existence of the anti and syn rotamers of 2- and 3-PCA has been confirmed by the matrix-isolation infrared spectroscopy along with the quantum chemical calculations. The anti and syn rotamers coexist in the Ar matrix immediately after the deposition for

3-PCA, while only the anti rotamer exists for 2-PCA.

3.2. Ratio of the rotamers for 3-PCA

The existence of the anti and syn rotamers has been confirmed for 2- and 3-PCA. If we assume only the conformational change between the two rotamers upon UV irradiation, then the increased amount of the syn rotamer should be the same as the decreased amount of the anti rotamer and vice versa. Thus, the population ratio of the two rotamers can be estimated from the infrared data obtained before and after the UV irradiation, based on the following relation:

$$\frac{N_{s'}}{N_{a'}} = -\left(\frac{I_{a''} - I_{a'}}{I_{s''} - I_{s'}}\right)\left(\frac{I_{s'}}{I_{a'}}\right), \qquad (1)$$

where N_x and I_x with $x = s$ (syn) and a (anti) denote, respectively, the population and the band intensity of one of the rotamers, and the prime and double prime denote the samples before and after the UV irradiation, respectively [6].

With 3-PCA, a pair of bands were examined for determining the population ratio, where the integrated band areas were obtained by a carve-fitting technique using Gaussian–Lorentzian functions. We have obtained the $N_{s'}/N_{a'}$ value of 0.16 for 3-PCA ($N_{s'}/N_{a'} = 0.57 \times (I_{1206}/I_{1215}) = 0.16$), which corresponds to the energy difference of 4.5 kJ mol^{-1} (376 cm^{-1}). This value is slightly large as compared with that obtained from the DFT calculation where the anti rotamer is more stable than the syn rotamer by 2.8 kJ mol^{-1} (234 cm^{-1}). The result that 3-PCA prefers the anti rotamer is consistent with that obtained previously using NMR and dipole-moment techniques [1–4]. Upon the UV irradiation of 3-PCA, other UV reaction processes such as decomposition might be responsible to yield wrong absorption coefficients, although the decomposition products could not be detected clearly in the present experiment.

With 2-PCA, the population ratio of the two rotamers could not be obtained using the relation (1), since the bands corresponding to the syn rotamer could not be detected in the matrix immediately after the deposition. In light of the output of the DFT calculation, the anti rotamer of 2-PCA was estimated to be energetically lower than the syn rotamer by 17.1 kJ mol^{-1} (1430 cm^{-1}) which corresponds to the anti/syn population ratio of 1/0.001 at 294 K.

3. 3. Intramolecular C–H···N hydrogen bonding of the anti rotamer of 2-PCA

In 1955, Pinchas investigated infrared spectra of a number of monosubstituted benzaldehydes and found a new kind of hydrogen bonding for ortho-substituted benzaldehydes, which gives rise to the blue-shift of the aldehyde C–H stretching band

[17–18]. The matrix-isolation infrared spectra of the aldehyde C–H stretching modes for 2- and 4-PCA in the 3000–2700 cm^{-1} region are shown in Fig. 5, where spectrum b is the difference spectrum; that is, the downward and upward bands are, respectively, due to the bands decreased and increased upon the UV irradiation. This observation shows that the observed bands are definitely assigned to each of the rotamers. Strong bands are observed separately in the 2859–2838 and 2749–2739 cm^{-1} regions, although the calculations show only one strong aldehyde C–H stretching band in the 2852–2793 cm^{-1} region. It is well known that the aldehyde C–H stretching mode and the first overtone of the aldehyde C–H in-plane deformation mode at about 1400 cm^{-1} are both in Fermi resonance [6,17,18,19]. In Table 4 we present the assignments of these vibrations based on the results of the calculations along with the infrared-band intensities. Several unassigned bands are also seen in Fig. 5. These bands are probably caused by the combination bands among the aldehyde CHO in-plane deformation and the ring vibration bands in the 1480–1410 cm^{-1} region and/or overtone bands of the ring vibration bands, whose modes are considerably mixed with the aldehyde CHO in-plane deformation mode. The observed small band splittings may be attributed to the site effects of the matrix [15]. The Fermi doublets are observed in the 2854–2817 and 2749–2739 cm^{-1} regions for the syn rotamer of 2-PCA and the syn and anti rotamers of 3-PCA as well as for 4-PCA. Thus, the intrinsic aldehyde C–H stretching band is estimated to be located around 2800 cm^{-1}. It has been reported by Green and Harrison [14] that the spectral patters in the above region of 3-and 4-PCA are very similar to each other, but the spectrum of 2-PCA shows the different pattern where the intensity of the 2710 cm^{-1} band is significantly lower [14]. We also have observed almost the same spectral feature for these molecules. Our interpretation for their observation is that the intramolecular C–H···N hydrogen-bonded C–H stretching band shifts to the higher wavenumber region resulting in the separation from the overtone band of the CHO deformation mode. Therefore, the former band observed at 2853 cm^{-1} exhibits no Fermi resonance with the latter overtone band at 2711 cm^{-1} for the anti rotamer of 2-PCA.

In order to clarify the characteristic tendency of the intramolecular C–H···N hydrogen bonding of the anti rotamer of 2-PCA, the aldehyde C–H and C=O stretching wavenumbers have been examined. In the geometry of the anti rotamer of 2-PCA optimized by the B3LYP/6-311++G(3df,2pd) level calculation, the aldehyde C–H bond length is shorter by 0.005 Å (1 Å = 10^{-10} m) than that of the syn rotamer (1.110 Å), where the aldehyde C–H bond length is 1.108–1.109 Å for both of the anti and syn rotamers of 3-PCA and for 4-PCA. The C–H···N distance of 2.514 Å for the anti

rotamer of 2-PCA is shorter than the sum of the van der Waals radii of H and N atoms (2.7 = (1.2 + 1.5) Å), though the C–H···N angle shows the acute angle of 70.9º. This result indicates the existence of the intramolecular C–H···N hydrogen bond. According to the Badger's rule, the stretching wavenumber is reciprocally proportional to the bond length [20–21]. Thus, the formation of the intramolecular C–H···N hydrogen bond for the anti rotamer of 2-PCA results in the shortening of the aldehyde C–H bond length, which gives rise to a blue-shift of the C–H stretching band. The comparison of the results of 2-PCA with those of 3- and 4-PCA shows that the C=O bond length is shortened by about 0.005 Å for the syn rotamer of 2-PCA, which is presumably caused by the repulsion between the N and aldehyde O atoms. In fact, the C=O stretching bands of the anti and syn rotamers of 2-PCA are observed at 1726 and 1738 cm^{-1}, respectively, which are in agreement with the calculated values of 1749 and 1768 cm^{-1}, indicating that the bond of the syn rotamer is more strengthened than that of the anti rotamer (see Table 3).

3. 4. Photolysis of 2-PCA

Figure 6 shows a difference spectrum of 2-PCA, where the spectrum observed immediately after UV irradiation ($\lambda \geq 300$ nm) is subtracted from that after UV irradiation without the short-wavelength cutoff filter. The bands denoted by asterisk and allow are newly observed ones along with the bands assigned to the syn rotamer. The assignments of the newly observed bands are carried out on the basis of the reported spectra. It is found that the band at 2138 cm^{-1} (asterisk) is associated with carbon monoxide [22] and that the bands at 1598, 1583, 1441, 1032, 992 and 701 cm^{-1} (allow**s**) are associated with pyridine [23]. These bands are detected only for 2-PCA upon UV or light irradiation ($\lambda < 370$ nm), but are not detected for 3- and 4-PCA.
It is noted that the increases of the band intensities of the less stable rotamer are also observed not by light irradiation with $\lambda > 420$ nm, but by UV or light irradiation ($\lambda <$ 370 nm) for both of 2- and 3-PCA. Therefore, the rotational isomerism of 2 and 3-PCA occurs not upon light irradiation with $\lambda > 420$ nm, but upon the UV or light irradiation with $\lambda < 370$ nm, although the energy of 420 nm light (285 kJ mol^{-1}) is high enough to pass through the rotational potential barrier (about 35 kJ mol^{-1}) in the ground state.
Table 4 shows the UV–VIS spectral data of 2-, 3- and 4-PCA in hexane at room temperature. The UV-VIS bands are observed in the wavelength region shorter than 400 nm. It is inferred from these data that the conformational change is taking place presumably via the electronically excited S_1 (n, π^*) and/or S_2 (π, π^*) states for both of 2- and 3-PCA. In particular for 2-PCA, the photoinduced rotational isomerism and

photolysis are detected simultaneously upon the UV or light irradiation ($\lambda < 370$ nm), although at present we could not identify whether these two processes occur simultaneously or consecutively.

4. Conclusions

Existence of the anti and syn rotamers has been confirmed for 2- and 3-PCA through the matrix-isolation infrared spectroscopy combined with the UV photoexcitation and the DFT calculations, and the observed bands for each rotamer have been assigned. The DFT calculations at the B3LYP/6-311++G(3df,2pd) level indicate that the anti rotamer exists predominantly for 2-PCA with the anti-syn energy difference of 17.1 kJ mol^{-1} (1430 cm^{-1}) and that the anti rotamer is slightly more stable than the syn rotamer by 2.8 kJ mol^{-1} (234 cm^{-1}) for 3-PCA. The anti and syn rotamers coexist in the Ar matrix immediately after the deposition for 3-PCA, while only the anti rotamer exists for 2-PCA. The results on the infrared-band intensity analyses for 3-PCA before and after the UV irradiation also show that the anti rotamer is lower in energy than the syn rotamer by 4.5 kJ mol^{-1} (376 cm^{-1}). Thus, both of the infrared data and the DFT calculations strongly support that the syn rotamer exists as a less stable isomer for 2- and 3-PCA. The aldehyde C–H wavenumber has been examined to clarify the characteristic tendency of the intramolecular C–H···N hydrogen bond of the anti rotamer of 2-PCA. It is shown that the formation of the intramolecular C–H···N hydrogen bond for the anti rotamer of 2-PCA results in the shortening of the aldehyde C–H bond length, which gives rise to a blue-shift of the C–H stretching band. The comparison of the data for 2-PCA with those for 3- and 4-PCA shows that the C=O bond length is shortened for the syn rotamer of 2-PCA, which is presumably caused by the repulsion between the aldehyde O and N atoms. With 2-PCA, photolysis takes place along with the photoinduced rotational isomerism to yield pyridine and carbon monoxide.

Acknowledgments

This work was supported in part by a Grant-in-Aid for Scientific Research (A) No. 16205003 from the Ministry of Education, Culture, Sports, Science and Technology of the Japanese Government. This work was also supported in part by a grant from the Hiruma

Foundation (Hamamatsu Photonics) through the president of Hiroshima University.

References

[1] L. Lunazzi, D. Macciantelli, G. Cerioni, J. Chem. Soc. Perkin Trans. 2, (1976) 1791.

[2] T. Drakenberg, J. Chem. Soc. Perkin Trans. 2, (1976) 147.

[3] W. Danchura, T. Schaefer, J. B. Rowbotham, D. J. Wood, Can. J. Chem., 52 (1974) 3986.

[4] J. S. Kwiatkowski, M. Swiderska, Bull. Acad. Pol. Sci. Ser. Sci. Chim., 25 (1977) 325.

[5] I. G. John, G. L. D. Ritchie, L. Radom, J. Chem. Soc. Perkin Trans. 2, (1977) 1601.

[6] T. Itoh, N. Akai, K. Ohno, J. Mol. Struct., in press.

[7] P. Felder, H. Hs. Guethard, Spectrochim. Acta, Part A, **36** (1980) 223.

[8] S. Kudoh, M. Takayanagi, M. Nakata, Chem. Phys. Lett., **296** (1998) 329.

[9] M. J. Frisch, G. W. Trucks, H. B. Schlegel, G.E. Scuseria, M. A. Robb, J. R. Cheeseman, J. A. Montgomery, Jr., T. Vreven, K. N. Kudin, J. C. Burant, J. M. Millam, S. S. Iyengar, J. Tomasi, V. Barone, B. Mennucci, M. Cossi, G. Scalmani, N. Rega, G. A. Petersson, H. Nakatsuji, M. Hada, M. Ehara, K. Toyota, R. Fukuda, J. Hasegawa, M. Ishida, T. Nakajima, Y. Honda, O. Kitao, H. Nakai, M. Klene, X. Li, J. E. Knox, H. P. Hratchian, J. B. Cross, C. Adamo, J. Jaramillo, R. Gomperts, R. E. Stratmann, O. Yazyev, A. J. Austin, R. Cammi, C. Pomelli, J. W. Ochterski, P. Y. Ayala, K. Morokuma, G. A. Voth, P. Salvador, J. J. Dannenberg, V. G. Zakrzewski, S. Dapprich, A. D. Daniels, M. C. Strain, O. Farkas, D. K. Malick, A. D. Rabuck, K. Raghavachari, J. B. Foresman, J. V. Ortiz, Q. Cui, A. G. Baboul, S. Clifford, J. Cioslowski, B. B. Stefanov, G. Liu, A. Liashenko, P. Piskorz, I. Komaromi, R.L. Martin, D.J. Fox, T. Keith, M.A. Al-Laham, C.Y. Peng, A. Nanayakkara, M. Challacombe, P. M. W. Gill, B. Johnson, W. Chen, M. W. Wong, C. Gonzalez, J. A. Pople, Gaussian 03, Revision B.05, Gaussian, Inc., Pittsburgh PA, 2003.

[10] A. D. Becke, J. Chem. Phys., **98** (1993) 5648.

[11] C. Lee, W. Yang, R. G. Parr, Phys. Rev. B, **37** (1988) 785.

[12] H. Yoshida, K. Takeda, J. Okamura, A. Ehara, H. Matsuura, J. Phys. Chem. A, **106** (2002) 3580.

[13] Y. Kawashima, M. Suzuki, K. Kozima, Bull. Chem. Soc. Jpn., 48 (1975) 2009.

[14] J. H. S. Green, D. J. Harrison, Spectrochim. Acta, Part A, 33A (1977) 75.

[15] D. Forney, M. E. Jacox, W. E. Thompson, J. Mol. Spectrosc., **157** (1993) 479.

[16] A. J. Barnes, J. Mol. Spectrosc., **113** (1984) 161.

[17] S. Pinchas, Anal. Chem., **29** (1957) 334.

[18] S. Pinchas, Anal. Chem., **27** (1955) 2.
[19] R. A. Nyquist, S. E. Settineri, D. A. Luoma, Appl. Spectrosc., **46** (1992) 293.
[20] E. Kurita, H. Matsuura, K. Ohno, Spectrochim. Acta, Part A, **60** (2004) 3013.
[21] R. M. Badger, J. Chem. Phys., **2** (1934) 128.
[22] H. Abe, K. M. T. Yamada, J. Chem. Phys., 121 (2004) 7803.
[23] S. Coussan, V. Brenner, J. P. Perchard, W. Q. Zheng, J. Chem. Phys., 113 (2000) 8059.

Figure captions

Fig. 1. Optimized geometries for 2-, 3- and 4-pyridinecarboxaldehyde. Nitrogen and oxygen atoms are indicated by black and hatched spheres, respectively. The bond lengths of the CHO group ($\times 10^{-10}$ m) at optimized geometries are indicated. The relative energies (kJ mol^{-1}) of the rotamers are given in parentheses.

Fig. 2. Observed (a) and calculated infrared spectra (b) of 4-pyridinecarboxaldehyde (4-PCA). The bands due to water in the matrix are indicated by asterisks.

Fig. 3. Observed and calculated infrared spectra of 3-pyridinecarboxaldehyde (3-PCA): a, spectrum observed immediately after the deposition of the sample at 15 K; b, the difference spectrum, where the spectrum obtained before the UV irradiation is subtracted from that obtained after the UV irradiation ($\lambda > 300$ nm); c, calculated spectrum, where the bands of the anti and syn rotamers are shown by the downward and upward bands, respectively. The bands due to water in the matrix are indicated by asterisks.

Fig. 4. Observed and calculated infrared spectra of 2-pyridinecarboxaldehyde (2-PCA): a, spectrum obtained immediately after the deposition of the sample at 15 K; b, the difference spectrum, where the spectrum obtained before the UV irradiation is subtracted from that obtained after the UV irradiation ($\lambda > 300$ nm); c, calculated spectrum, where the bands of the anti and syn rotamers are shown by the downward and upward bands, respectively. The bands due to water in the matrix are indicated by asterisks.

Fig. 5. Observed infrared spectra of 2- and 4-pyridinecarboxaldehyde (2- and 4-PCA) in the aldehyde C–H stretching region: a, the spectrum of 2-PCA; b, the difference spectrum of 2-PCA, where the spectrum obtained before the UV irradiation is subtracted from that obtained after the UV irradiation ($\lambda > 300$ nm); c, the spectrum of 4-PCA.

Fig. 6. Difference spectrum of 2-pyridinecarboxaldehyde (2-PCA), where the spectrum obtained after the UV irradiation ($\lambda > 300$ nm) is subtracted from that obtained after the UV irradiation without the short-wavelength cutoff filter for 10 min. The bands due to carbon monoxide and pyridine are indicated by asterisk and arrows,

respectively.

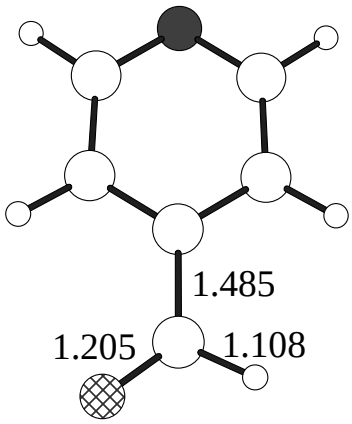

4-Pyridinecarboxaldehyde (4-PCA)

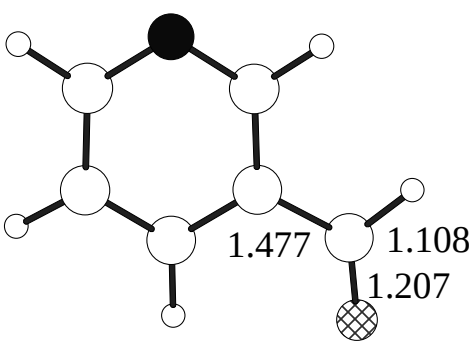

Anti (0.0)

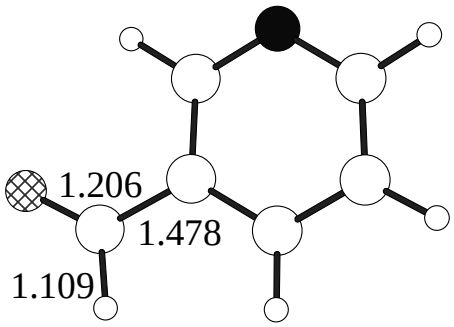

Syn (2.8)

3-Pyridinecarboxaldehyde (3-PCA)

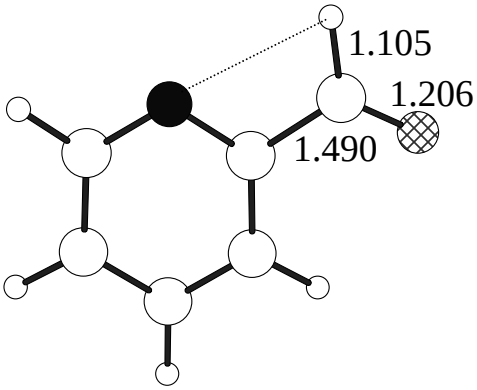

Anti (0.0)

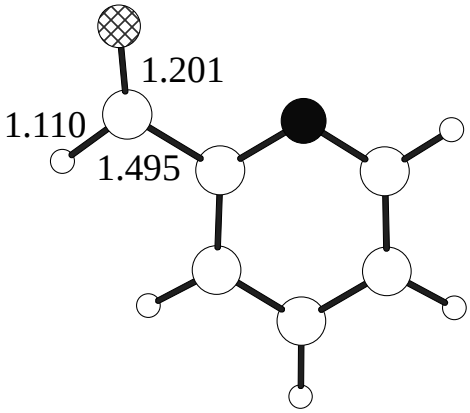

Syn (17.1)

2-Pyridinecarboxaldehyde (2-PCA)

Fig. 1. K. Ohno et al.

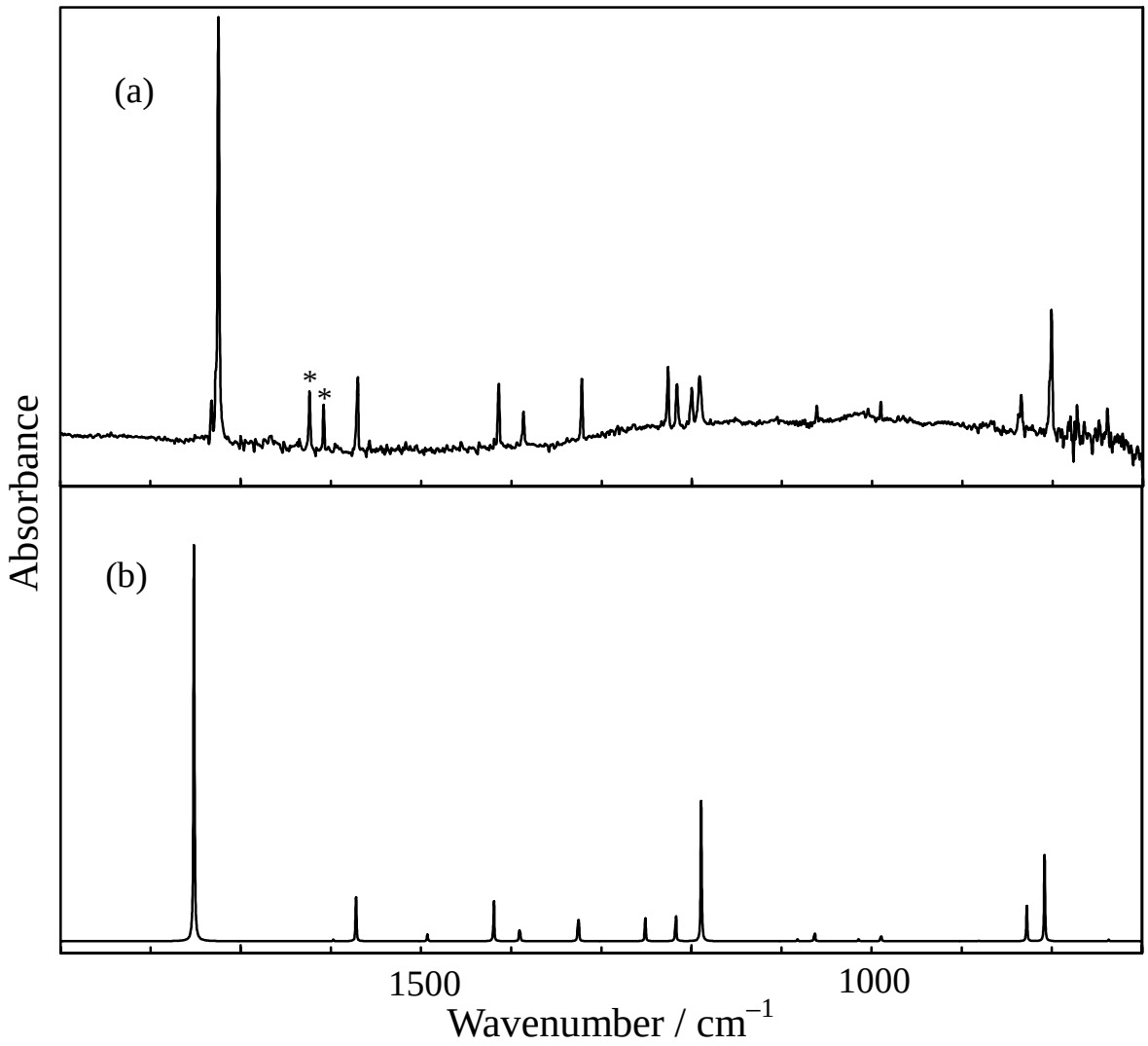

Fig. 2. K. Ohno et al.

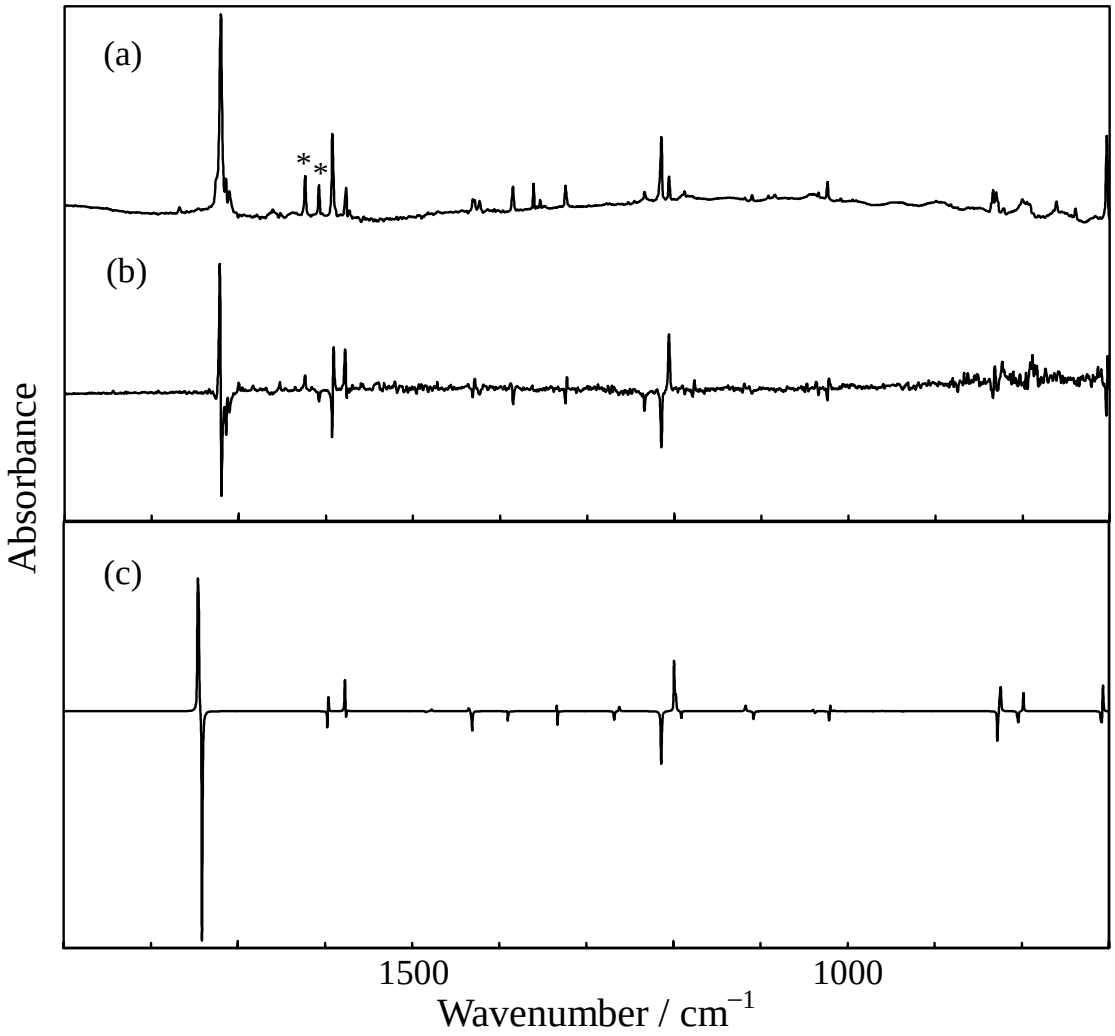

Fig. 3. K. Ohno et al.

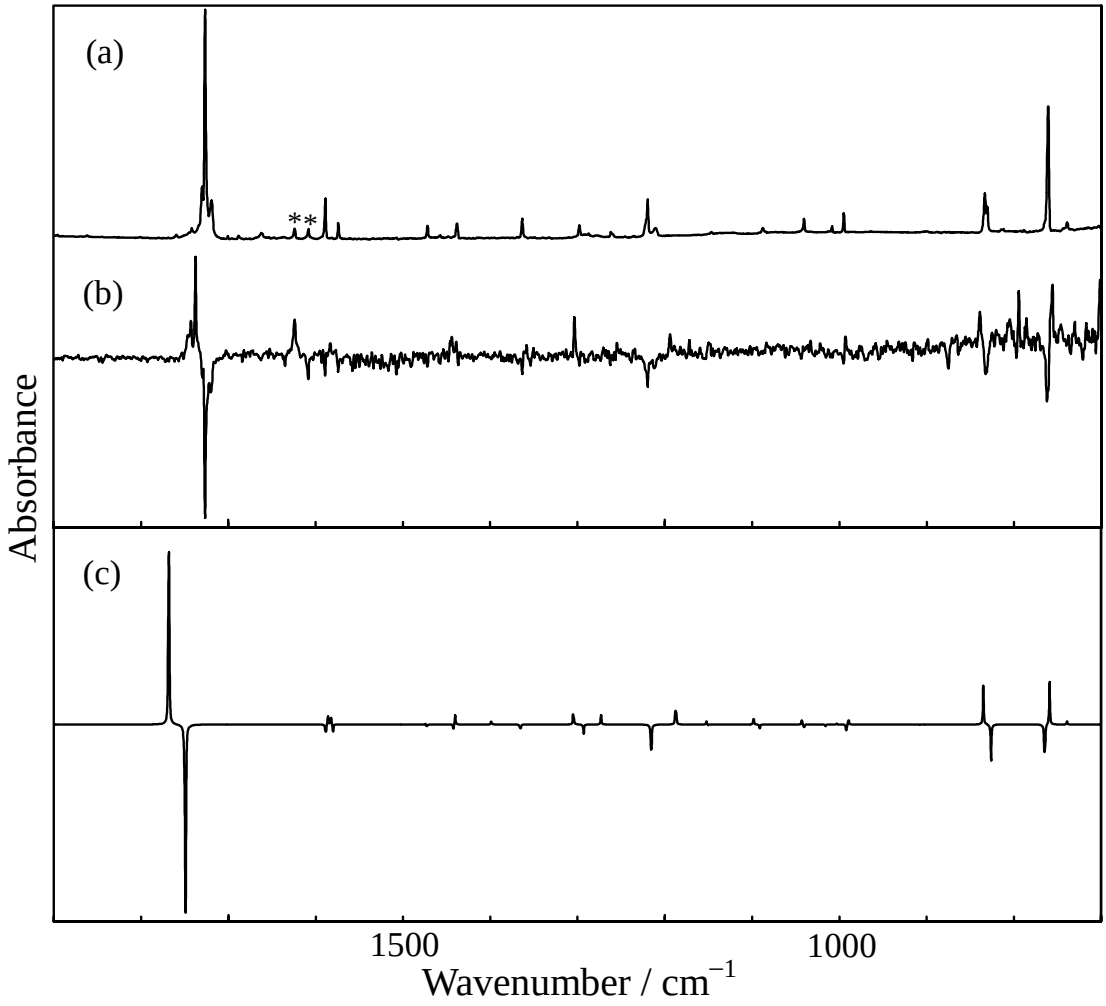

Fig. 4 K. Ohno et al.

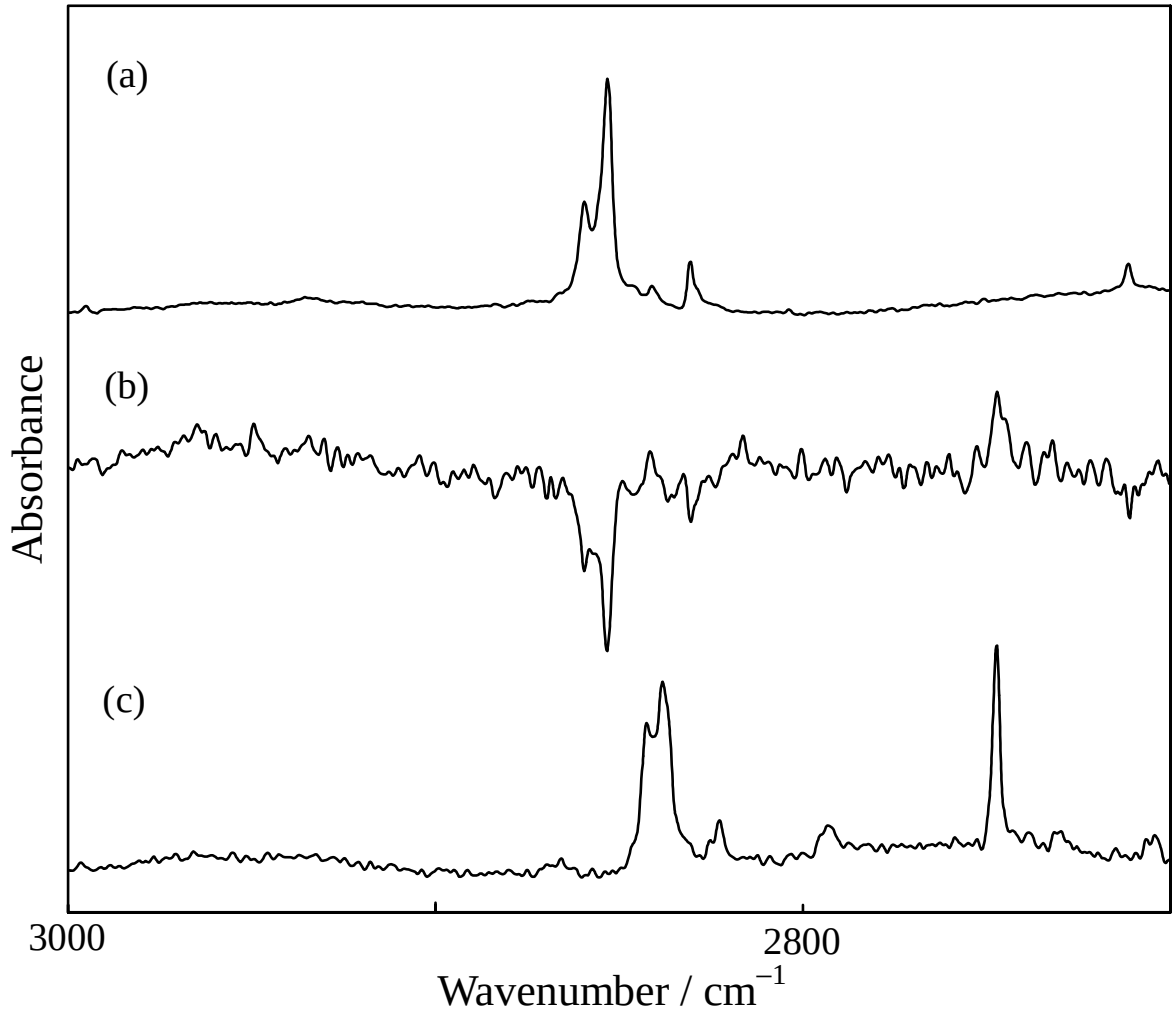

Fig. 5. K. Ohno et al.

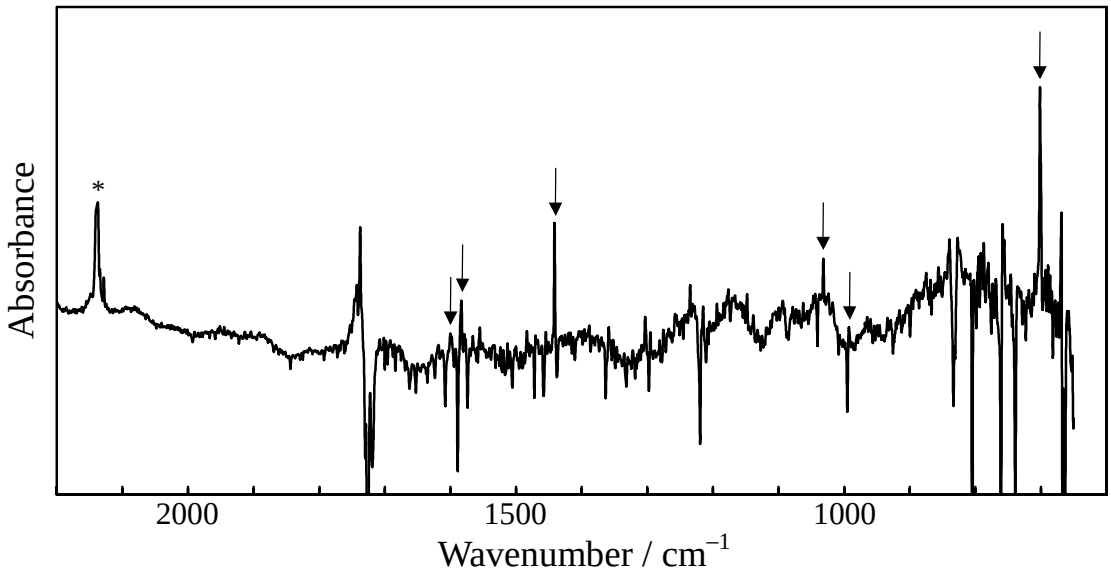

Fig. 6. K. Ohno et al.

Table 1
Observed and calculated wavenumbers of 4-PCA

Obs/cm^{-1}	Int[a]	Calc/cm^{-1}	Int[b]	Assignment[c]
1725	vvs	1752	239	C=O str (ip)
1595	vw	1597	1	Ring (ip)
1570	s	1572	22	Ring (ip)
1506	w	1493	3	Ring (ip)
1414	s	1419	19	Ring (ip)
1387	m	1391	8	CHO def (ip)
1322	s	1325	16	CH def (ip)
1226	s	1251	13	Ring (ip)
1216	s	1217	16	CH def (ip)
1200	s			Com (989 + 210)
1191	s	1189	64	Ring (ip)
1085	vw	1082	1	CH def (ip)
1062	w	1063	6	CH def (ip)
1004	vw	1015	1	CHO def (op)
		996	0	CH def (op)
991	w	989	3	Ring (ip)
		973	0	CH def (op)
		881	0	CH def (op)
835	m	828	15	CC str (ip)
801	vs	808	37	CH def (op)
739	w	737	1	Ring (op)
668	w	666	1	Ring (ip)
647	vs	646	38	Ring (ip)

Bands in the 1800–600 cm^{-1} region are listed.
Calculations at the B3LYP/6-311++G(3df,2pd) level.

[a] Int: vvs, very very strong; vs, very strong; s, strong; m, medium; w, weak; vw, very weak.

[b] Int: intensity in km mol^{-1}.

[c] Brief assignments are shown: C=O str, C=O stretching; ring, stretching and/or bending of the pyridine ring (Py); CH def, CH deformation; CC str, CC stretching of Py-CHO bond; ip, in-plane mode; op, out-of-plane mode, Com: combination band that is intensified by Fermi resonance with the 1191 cm^{-1} band [14].

Table 2
Observed and calculated wavenumbers of 3-PCA

Obs/cm^{-1}		Calc/cm^{-1}				Assignment[a]
	Int[b]	Anti[c]	Int[d]	Syn[c]	Int[d]	
1722	vvs			1746	264	C=O str (ip)
1720	vvs	1741	264			C=O str (ip)
1593	m	1596	87			Ring (ip)
1591	vs			1596	73	Ring (ip)
1578	s			1577	43	Ring (ip)
1576	vw	1576	18			Ring (ip)
1473	vw	1484	2	1478	3	Ring (ip)
1431	w	1431	24			CH def (ip)
1429	w			1435	7	CH def (ip)
1388	s			1390	8	CHO def (ip)
1385	s	1390	16			CHO def (ip)
1325	s	1333	17			CH def (ip)
1323	s			1334	11	CH def (ip)
		1268	9	1262	6	Ring (ip)
1215	vs	1214	61			CH def (ip)
1206	s			1199	52	Ring (ip)
				1197	21	CH def (ip)
		1191	7			Ring (ip)
1119	vw			1117	9	CH def (ip)
1111	vw	1108	10			CH def (ip)
1037	vw			1040	2	Ring (ip)
1035	vw	1037	2			Ring (ip)
1024	m	1021	11			Ring (ip)
1022	m			1020	10	Ring (ip)
		1019	1	1015	1	CHOdef (op)
		1002	0	997	0	CH def (op)
		971	0	960	0	CH def (op)
		937	0	950	0	CH def (op)
834	m	828	37			CC str (ip)
832	m			824	44	CC str (ip)
805	w	804	18			CH def (op)
796	w			798	19	CH def (op)
704	s	708	29			Ring (op)
703	s			707	31	Ring (op)
668	m	671	19	663	29	Ring (ip)
		618	3	617	2	Ring (ip)

Bands in the 1800–600 cm^{-1} region are listed.
Calculations at the B3LYP/6-311++G(3df,2pd) level.

[a] Brief assignments are shown: C=O str, C=O stretching; ring, stretching and/or bending of the pyridine ring (Py); CH def, CH deformation; CC str, CC stretching of Py-CHO bond; ip, in-plane mode; op, out-of-plane mode.

[b] Int: vvs, very very strong; vs, very strong; s, strong; m, medium; w, weak; vw, very weak.

[c] As for geometries, see Fig. 1.

[d] Int: intensity in km mol^{-1}.

Tbale 3
Observed and calculated wavenumbers of 2-PCA

Obs/cm^{-1}	Calc/cm^{-1}				Assignment[a]
Int[b]	Anti[c]	Int[d]	Syn[c]	Int[d]	
1738 s			1768	246	C=O str (ip)
1726 vs	1749	237			C=O str (ip)
1589 s	1588	15			Ring (ip)
1583 vw			1586	10	Ring (ip)
1574 w	1580	9	1582	11	Ring (ip)
	1472	2	1474	1	Ring (ip)
1441 w			1440	12	CH def (ip)
1438 w	1442	5			CH def (ip)
1391 vw			1399	5	CHO def (ip)
1363 w	1365	6			CHO def (ip)
1304 m			1305	17	CH def (ip)
1298 w	1293	9			CH def (ip)
	1277	0			Ring (ip)
			1273	11	Ring (ip)
1219 s	1216	49			Ring (ip)
1194 w			1188	26	Ring (ip)
1149 vw			1152	4	CH def (ip)
1147 vw	1150	1			CH def (ip)
1088 vw	1091	4	1098	8	CH def (ip)
			1043	6	Ring (ip)
1040 w	1040	4			Ring (ip)
1008 vw	1016	2	1003	1	CHO def (op)
	1005	0	998	0	CH def (op)
995 m	992	7			Ring (ip)
992 w			989	8	Ring (ip)
	971	0	968	0	CH def (op)
	908	0	899	0	CH def (op)
839 m			835	41	CC str (ip)
834 s	826	36			CC str (ip)
761 vs	765	48			CH def (op)
756 s			759	46	CH def (op)
739 vw	740	1	739	5	Ring (op)
669 s			673	28	Ring (ip)
663 s	665	26			Ring (ip)
	614	14	619	4	Ring (ip)

Bands in the 1800–600 cm^{-1} region are listed.
Calculations at the B3LYP/6-311++G(3df,2pd) level.

[a] Brief assignments are shown: C=O str, C=O stretching; ring, stretching and/or bending of the pyridine ring (Py); CH def, CH deformation; CC str, CC stretching of Py-CHO bond; ip, in-plane mode; op, out-of-plane mode.

[b] Int: vvs, very very strong; vs, very strong; s, strong; m, medium; w, weak; vw, very weak.

[c] As for geometries, see Fig. 1.

[d] Int: intensity in km mol^{-1}.

Table 4
Observed and calculated wavenumbers of the aldehyde CH stretching

	Obs/cm^{-1}	Int[a]	Calc/cm^{-1}[b]	Assignment
2-PCA				
	2859	m		2×Ring (Anti; 2×1438 = 2876)
	2853	s	2852	CH stretching (Anti)
	2831	w		Combination (Anti; 1472 + 1363 = 2835)
	2817[c,d]	vw		2×CHO deformation (Syn; 2×1391 = 2782)
	2747[c,d]	w	2786	CH stretching (Syn)
	2711	vw		2×CHO deformation (Anti; 2×1363 = 2726)
3-PCA				
	2854[d]	s	2812	CH stretching (Anti)
	2842[d]	s		
	2838[d]	s	2793	CH stretching (Syn)
	2800	m		Combination (Syn; 1429 + 1388 = 2817)
	2749[d]	m		2×CHO deformation (Anti; 2×1385 = 2770)
	2743[d]	m		
	2739[u]	m		2×CHO deformation (Syn; 2×1388 = 2776)
4-PCA				
	2843[d]	m	2811	CH stretching
	2838[d]	s		
	2823	w		2×Ring (2×1414 = 2828)
	2793	w		Combination (1414 + 1387 = 2801)
	2747[d]	s		2×CHO deformation (2×1387 = 2774)

[a] Int: s, strong; m, medium; w, weak; vw = very weak.

[b] The wavenumbers calculated at the B3LYP/6-311++G(3df,2pd) level are scaled by 0.97.

[c] The band is newly observed by UV irradiation.

[d] The bands are in Fermi resonance.

Table 5

UV−VIS spectroscopic data for pyridinecarboxaldehyde in hexane at room temperature

State	Location			Molar extinction coefficient
	cm^{-1}		nm	
2-PCA				
$S_2(\pi, \pi^*)$	37400	(Max)	267.4	3700
$S_1(n, \pi^*)$	26430	(Origin)	378.4	7.9
$T_1(n, \pi^*)$	24500	(Origin)	408.2	0.11
3-PCA				
$S_2(\pi, \pi^*)$	37240	(Max)	268.5	3100
$S_1(n, \pi^*)$	26510	(Origin)	377.2	5.9
$T_1(n, \pi^*)$	24780	(Origin)	403.6	0.12
4-PCA				
$S_2(\pi, \pi^*)$	35300	(Max)	283.3	5500
$S_1(n, \pi^*)$	26200	(Origin)	381.7	14.1
$T_1(n, \pi^*)$	24310	(Origin)	411.4	0.18